SciMedCentral

Chemical Engineering & Process Techniques

Research Article

Fabrication of 3D-Bioprinted Polyurethane/Chitosan-Based Scaffold for Annulus Fibrosus Tissue Engineering: *In Vitro* Study

Aboulfazl Barati[1,4*], Mostafa Esmaeilpour[1], Javad Esmaeili[1,2], Mehdi Salehiamin[2,3] and Mitra Pakrouyan[1]

[1]*Departments of Chemistry and Physics, Troy University, USA*
[2]*Department of Tissue Engineering, TISSUEHUB Co, Iran.*
[3]*Department of Anatomy, Tehran University of Medical Sciences, Iran*
[4]*College of Arts and Sciences, University of Troy, USA*

***Corresponding author**

Aboulfazl Barati, Center for Materials and Manufacturing Sciences, Departments of Chemistry and Physics, Troy University, Troy, Alabama 36082, USA

Submitted: 30 June 2024

Accepted: 31 July 2024

Published: 02 August 2024

ISSN: 2333-6633

Keywords

- Annulus fibrosus
- Chitosan
- 3D Bioprinting
- Polyurethane
- Tissue engineering

Abstract

Low back pain is frequently associated with disc degeneration, which is being treated through tissue engineering of the annulus fibrosus (AF). This study aimed to utilize 3D bioprinting to fabricate a chitosan-coated Polyurethane (PU)-based scaffold (PUCh) for AF tissue engineering with suitable biological, physical, and mechanical properties. PU scaffolds were fabricated by depositing PU struts at 90°/0° towards the horizontal surface. For biocompatibility purposes, PU scaffolds were coated with different content of chitosan (0, 1, 2.5, and 5 %). The scaffold morphology, surface roughness, mechanical strength, degradation, as well as biocompatibility were characterized. Overall, PUCh indicated appropriate surface roughness, elastic modulus (1.25 MPa), swelling ratio (50%), and degradation rate (3.56 %), subsequently having a high level of biocompatibility (94 %). The presence of Ch reduced the space between the struts. In conclusion, PUCh can be considered in AF tissue engineering after suitable modification.

INTRODUCTION

Lower back pain (LBP) is a widespread musculoskeletal disorder that can result in disability and enforce a socio-economic encumbrance [1,2].intervertebral disc (IVD) degeneration and disc herniation are the predominant reasons for LBP in middle-aged and elderly people, which considerably affects the quality of life [3,4]. At present, discectomy is the most common surgical treatment for disc herniation. Although removing the herniated nucleus pulposus (NP) tissue leads to relieving clinical symptoms, the annulus fibrosus (AF) defect is not treated by this procedure. Untreated AF defects are known as a main cause of postoperative consequences containing, but not limited to chronic low back pain, decrease in disc height, progressive disc degeneration, and recurrent herniation [5,6]. Indeed, there is an obvious crack in current surgical treatment which drives researchers to develop new treatment procedures for AF defect restoration to promote the quality of patient life.

Tissue engineering offers prodigious assurance to make a new tissue-engineered composite disc in which there is a potential to restore native disc structure, biology, and mechanical properties. Tissue engineering is a promising technique to treat AF defects and advanced IVD degeneration that requires surgical intervention [7,8]. To treat AF defects and end-stage IVD degeneration, considerable scaffolds have been developed via various techniques.

Diverse techniques have been used for the fabrication of the 3D scaffolds, containing the leaching method [9]; solvent castings [10]; phase separation [11]; freeze-drying [12]; stereolithography [13]; melt electro-writing (MEW) [14]; electrospinning [15]; and wet spinning [16]; to IVDs regeneration and repair. The emergent 3D printing technology is one of those that offers noteworthy benefits in the fabrication of personalized complicated structures and organs. Scaffolds through 3D bioprinting for AF defects can be made from both natural and synthetic materials.

Although synthetic polymer materials have the necessary mechanical properties, they lack an environment that improves cell activity [17]. Since AF tissue has mechanical and tensile properties, it is recommended to employ hybrid scaffolds. A tissue-engineered substitute for AF defect should not only provide mechanical support but also create a suitable environment for living cells after being implanted at the IVD site. Additionally, natural polymers have the potential to imitate the extracellular matrix found in natural AF by establishing a microenvironment that is both supportive to cells and has low toxicity, resulting in improved cell compatibility [18]. As a replacement for AF in tissue engineering, it is anticipated that it will offer adequate

mechanical support and a conducive environment for living cells after being implanted at the IVD site. Therefore, using a combination of synthetic and natural polymers to create scaffolds for AF defects would be an effective approach [19,18].

For instance, Chen Liu et al. found that poly(ester carbonate urethane)urea (PECUU) mimics the natural AF ECM's mechanical properties, but lacks its biological activity. The decellularized AF matrix (DAFM), which is biocompatible and biodegradable and promotes ECM secretion, was used to create a hybrid electrospinning scaffold using coaxial electrospinning technology. Results showed that the gene expression and ECM secretion of type I and II collagens and proteoglycan from annulus-derived stem cells cultured on the DAFM/PECUU scaffold were higher than that on the PECUU scaffold alone [20]. In another study, Ankush Dewle and his colleagues revealed that aligned-polycaprolactone (PCL) nanofibers when crosslinked with an electro-compacted type-I collagen patch, showed more hydrophilic, rough-nano features. The composite provided ample ligands for cell attachment supporting the adequate proliferation of primary goat annulus fibrosus (AF) cells and also favored sufficient production of collagen type-I and a glycosaminoglycan extracellular matrix as compared to other groups [21].

Despite the encouraging results from several studies in the field of tissue engineering utilizing 3D-printed AF, regenerating AF remains a significant challenge [22-24]. Based on our literature review, numerous studies demonstrate the effectiveness of hybrid scaffolds in comparison with single ones (synthetic or natural) [25-27]. The objective of this research was to manufacture a unique composite material combining synthetic and natural polymers using 3D-bioprinting technology. Polyurethane (PU) for its mechanical and elasticity, and chitosan (Ch) for its biocompatibility properties were chosen. This study aimed to investigate the quality of the hybrid PU/Ch scaffold for AF tissue engineering.

METERIALS&METHODS

Materials

Chitosan (Ch) with medium molecular weight (deacetylation degree of 75-85%, Sigma-Aldrich), sodium hydroxide (NaOH), Acetic acid, Phosphate buffer saline (PBS, Mojalali), Tripolyphosphate (TPP, Sigma-Aldrich), Polyurethane (PU), were provided from a local supplier. NIH/3T3 cell lines were purchased from the Pasteur Institute of Iran.

AF scaffold design

The dimensions of IVD were obtained from a 47-year-old male patient through MRI images of 1-2 lumbar disc levels. The three-dimensional intervertebral disk model was isotropically resized to half. The scaffold was designed in a way of intermittent fibers with an angle of 0°/90°. The diameter of the fibers was adjusted to 300 µm. By utilizing SolidWorks software, a 3D model of annulus fibrosus was designed.

Scaffold fabrication

3D printing of Polyurethane scaffold: 20 gr PU granules were added to the extrusion cylinder of 3D bioprinting (BIOFABX2, OMID AFARINAN company). For polymer printing, the PU scaffold was deposited using a 300-µm nozzle at a speed of 6 mm/min at 150 °C.

Chitosan solution: Preparing 1, 2.5, and 5 % (w/v) of the aqueous solution of Ch powder, Ch powder was dissolved in 1 % (v/v) acetic acid and stirred at 500 rpm for 5 h to acquire a homogenous solution.

PU scaffolds coated with Ch: For this aim, three custom molds with paste were prepared and covered with a thin layer of LDPE to prevent the penetration of Ch solution into the molds, and the scaffolds were placed in the molds. Then, different solutions of Ch were poured into the molds and left for 2 h to cover the PU scaffolds. Next, sodium tripolyphosphate (TPP) solution was added to each mold as a cross-linking agent and left for 24 hours to form links. In the end, we had three different PU scaffolds coated with 1, 2.5, and 5 % of Ch (PUCh-1, PUCh-2.5, and PUCh-5, respectively).

SEM

To analyze the morphology and microstructures of the scaffolds, they were coated with a layer of gold employing a spotting coater. Then scanning electron microscopy (SEM) (Philips XL30; Philips, Eindhoven, Netherlands) was conducted under a 25 kV accelerated voltage.

FTIR

Fourier transform infrared spectroscopy (FT-IR) was used to characterize the chemical structure of the fabricated PU and PUCh scaffold. The attenuated total reflectance-Fourier transform infrared (ATR-FTIR) device (Nicolet 10, Thermoscientific) recorded transmittance of the scaffolds in the range of 400-4000 cm-1 and 4 cm-1 resolution.

Tensile test

A universal testing machine (SANTAM, STM-20, Iran) was used to measure the tensile properties of the scaffold. The samples were pulled at a constant rate of 5 mm/min following ASTM D638. Ultimate tensile strength, elongation at break, and tensile modulus were reported. The area of the samples was measured by SolidWorks software (version SP0.1) which was equilibrium to 279 square mm.

Swelling

First, the dried scaffold was weighed (W0) and then immersed in PBS solution at room temperature for 24 hrs. The swollen scaffold was removed and the excessive water was removed from the scaffold surface using filter paper. Finally, the scaffold was weighed again (W1). The swelling ratio was measured using the formula:

$$Swelling(\%) = \frac{W_1 - W_0}{W_0} \times 100 \quad (1)$$

Porosity

The porosity of the scaffolds was determined using the liquid displacement method and ethanol was used as the alternative liquid. Ethanol was chosen as it quickly diffuses into the scaffolds without causing any dissolving or swelling of the scaffold or changing its structure. To determine the porosity, a certain amount of ethanol was added to a 10 mL graduated cylinder (V0) and the scaffold was then immersed in 96% ethanol for 5 minutes to remove air bubbles. The final stable volume of ethanol in the cylinder was recorded (V1). After removing the scaffolds from the ethanol, any residual ethanol on its surface was wiped off and the final volume of ethanol in the cylinder was recorded (V2). The porosity rate was determined as follows:

$$Porosity(\%) = \frac{(V_0 - V_2)}{(V_1 - V_2)} \times 100 \quad (2)$$

Degradation

The scaffolds were weighed as an initial weight (Wi). Then, they were immersed in PBS solution at a pH of 7.4 at 37 °C. A series of nine sequential weight measurements were taken of scaffolds after being removed from the PBS solution, thoroughly washed with deionized water, and then freeze-dried. The intervals between each measurement were seven days in duration. The final weight of the scaffolds was recorded as Wf. The scaffold degradation rate was calculated through the following equation:

$$Degradation(\%) = \frac{W_i - W_f}{W_i} \times 100 \quad (3)$$

MTT

The biocompatibility of the scaffolds was investigated by employing an MTT test. First, scaffolds were immersed in ethanol (96%) for 24 h. Following drying the scaffolds through freeze-drying, the samples were sterilized under a UV ray for 1 h. Then, every scaffold was planted with 1 × 104 fibroblast cells (NIH/3T3 cell line). Next, the samples were incubated at 37 °C and 5% CO2 for 24 h. After 24 h incubation, 100 µl MTT solution (5 mg/ml in PBS) was added to each well and incubated for 4 h until MTT formazan was made. Next, after aspiration of supernatant, 100 µl of DMSO was added to each well followed by sufficient pipetting to dissolve the MTT formazan crystals. Finally, the resultant soluble was centrifuged at 1500 rpm for 5 min. The supernatant was transmitted to a 96-well plate and read via ELISA reader at a wavelength of 570 nm. The test was performed in triplicate.

Statistical analysis

The quantitative data were stated as means ± SD and analyzed using one-way and two-way ANOVA with subsequent Tukey's post-hoc tests. Statistical analyses were conducted utilizing GraphPad Prism, version 9.0.0. A $p < 0.05$ was considered to be a statistically significant difference.

RESULTS

In this study, we designed a new 3D-bio printed scaffold from PU coated with different amounts of Ch (1, 2.5, and 5%) for annulus fibrosus tissue. First, we designed a 3D model of annulus fibrosus by using SolidWorks software. Then, the PU scaffold was fabricated via 3D bioprinting and then coated with different % mass of Ch to improve biocompatibility properties. PU scaffold coated with Ch cross-linked with TPP [Figure 1].

Morphological analysis

Surface morphologies of the PU scaffold and PUCh scaffolds of SEM images are presented in Figure 2. As can be seen in Figure 2A-a, the PU scaffold had a smooth surface, but the scaffold coated with chitosan showed a rough surface and contained microporous structures [Figure 2A-b]. Figure 2B indicates that PU scaffolds which are coated with 1, 2.5, and 5% of Ch, have gradually decreased porosity as can be seen in Figures 2B-a, b, and c, respectively. Through increasing the mass of Ch in PU scaffolds, the roughness was decreased gradually [Figure 2C-a, b, and c].

FTIR

Figure 3 represents FTIR spectra of pure PU and Ch materials and PUCh scaffolds. Absorption bands in CH represent -OH at 3200-3650 cm-1, -NH (amide II) between 1550-1600 cm-1, amide II at 1625 cm-1, and C=O (carbonyl) at 1650-1780 cm-1. Considering the PU scaffold, the absorption band which appears at 3300 cm-1 is assigned to -NH. The peak at 1712 cm-1 is characteristic of the stretching vibration of C=O. Sharp peaks at 2859 and 2938 cm-1 are assigned to stretching -CH2. The Peak existing at 2882 cm-1 represents symmetric -CH3. There are some molecular interactions between Ch and PU. The stretching peak at 3346 cm-1 in the PUCh scaffolds shows

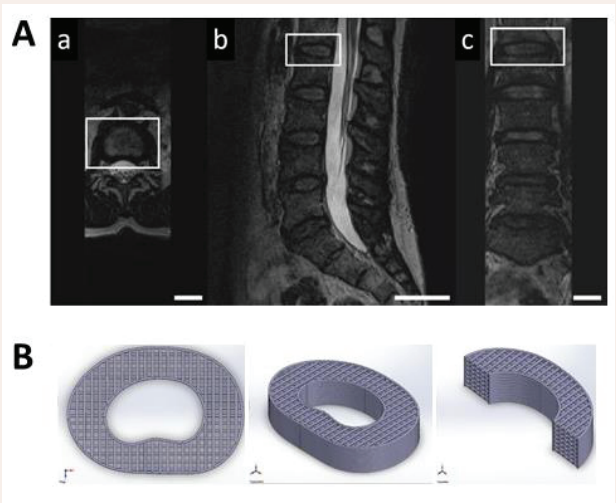

Figure 1 A) MRI images of the patient. Images taken from the transverse (a), sagittal (b), and frontal (c) planes. The intervertebral disc between L1-L2, was displayed through white rectangle (scale bars: 4 cm). B) Different views of fibrous annulus 3D model designed by SolidWorks software.

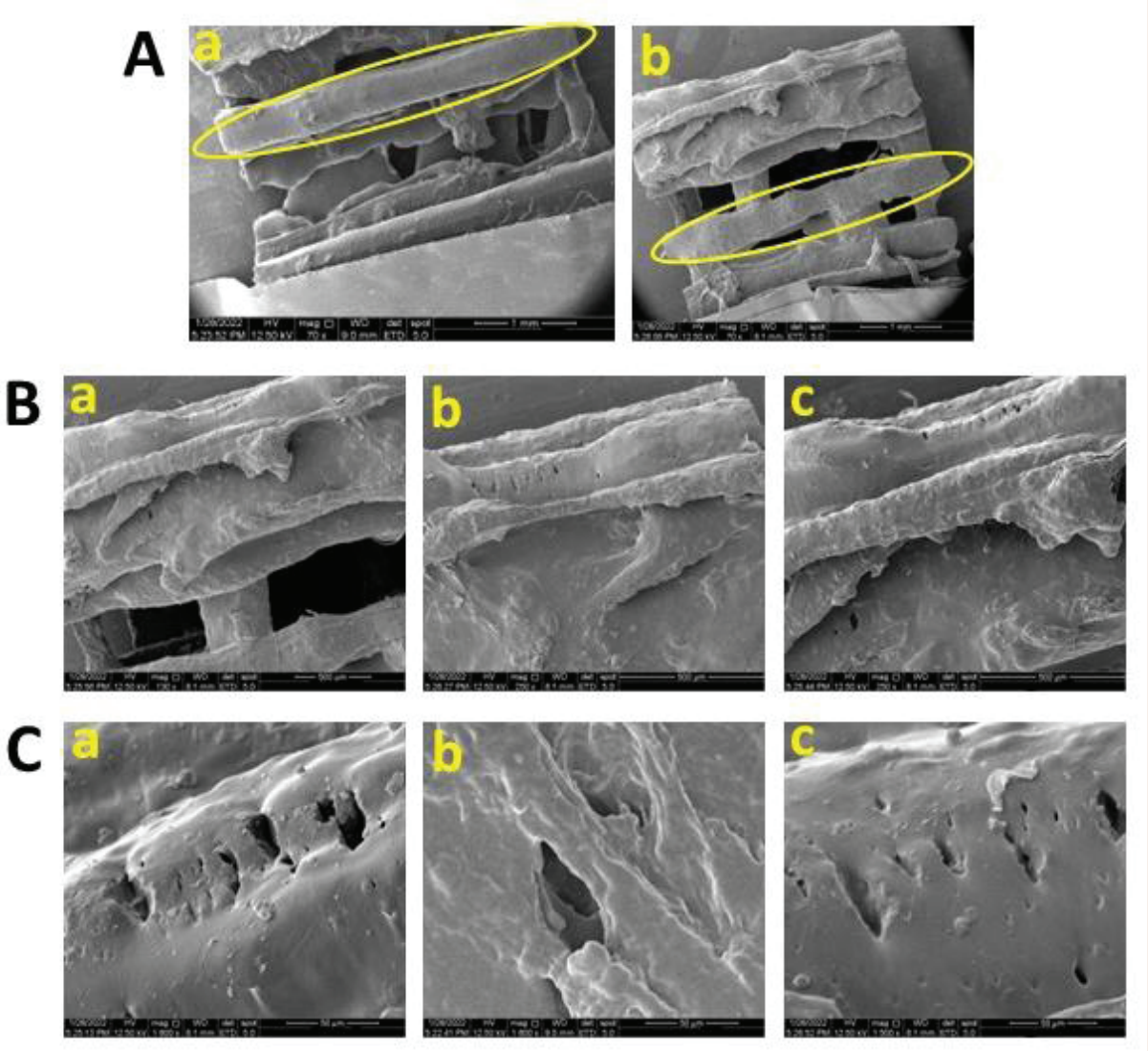

Figure 2 A) SEM images of PU and CH-coated PU scaffolds. B) Microstructures of PU scaffolds coated with 1 (a), 2.5 (b), and 5 (c) % of chitosan. C) surface stiffness of PU scaffolds with different chitosan mass (1 (a), 2.5 (b), and 5 (c) %).

the presence of chitosan in PU scaffolds which is owing to N-H stretching vibration. The appearance of this peak was expanded by increasing the amount of chitosan in the PU scaffold. Also, the band that appeared at 1651 cm-1 is assigned to -NH (amide I) which is in all PUCh scaffolds, representing the presence of chitosan in PU scaffolds.

Mechanical strength

The outcomes from tensile strength demonstrated the mechanical properties of PU scaffold and PUCh scaffolds in Figure 4. Based on Figure 4A, the tensile modulus was significantly

different between PU and PUCh-5 scaffolds ($p < 0.05$). Moreover, the tensile strength of the PU scaffold was significantly lower than the PUCh-2.5 ($p < 0.0003$) and PUCh-5 ($p < 0.0001$) scaffolds [Figure 4B].

Swelling analysis

The swelling rate of the scaffolds with different ratios of chitosan is reported in Figure 5A. The results indicated that the PU scaffold had the least swelling behavior in comparison with the PUCh-1 ($p < 0.0029$), PUCh-2.5, and PUCh-5 ($p < 0.0001$) scaffolds. Moreover, PU scaffolds with an increased mass of Ch, demonstrated a gradually increased swelling rate, and PUCh-5 had a significant difference compared with PUCh-2.5 and PUCh-5 ($p < 0.0001$).

Porosity

As shown in Figure 5B, the porosity of the pure PU scaffold was higher (27.11%), and the porosity of PU scaffolds gradually decreased after coating with increasing content of chitosan (1, 2.5, and 5%), indicating the porosity rate of 17.02, 13.84, 10.25

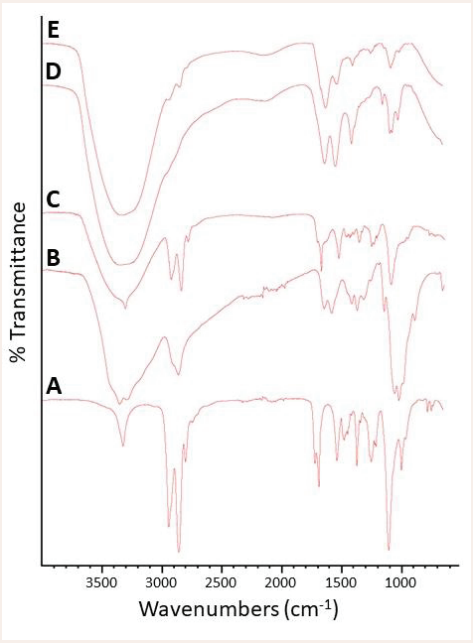

Figure 3 The FTIR Spectra of PU and PUCh scaffolds.

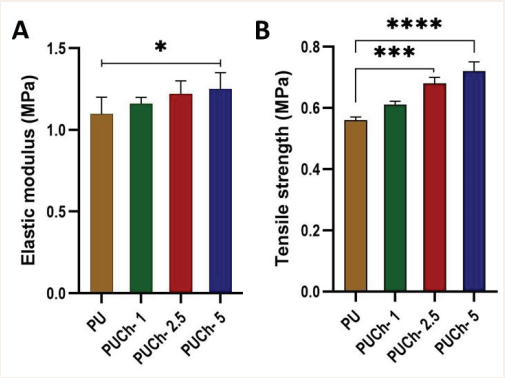

Figure 4 Indicates the elastic modulus (A) and tensile strength (B) properties of the scaffolds.

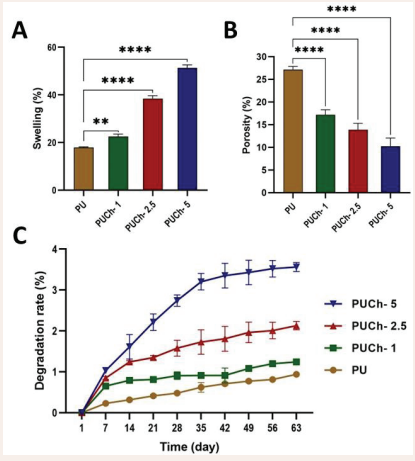

Figure 5 A) Swelling behavior of the scaffolds. B) The porosity of the scaffolds. C) Degradation behavior of the scaffolds.
(**, p < 0.0029; ****, p < 0.0001).

%, respectively. Indeed, the PU scaffold was higher than scaffolds coated with 1, 2.5, and 5 % of chitosan ($p < 0.0001$). Furthermore, PUCh-5 had the lowest porosity rate in comparison with PUCh-2.5 ($p < 0.038$) and PUCh-1 ($p < 0.0009$).

Degradation

Figure 5C shows the degradation rate of pure PU scaffolds and PUCh scaffolds with different content of chitosan over 63 days. The pure PU scaffold degraded 0.94% by weight after

63 days in a very slow and stable manner. PU coated with 1, 2.5, and 5% of chitosan showed an increasing degradation rate with a degrading %mass of 1.24, 2.13, and 3.56, respectively. PUCh-5 scaffold had a steep gradient until the 35th day than other scaffolds and then became the same as other ones.

MTT

To evaluate the viability of the scaffolds, an MTT test was utilized. As can be seen, the PU scaffold indicated a low percentage of cell viability (88.1 %) and the statistical analysis stated the significant difference between the PU scaffold and PUCh-1, PUCh-2.5, and PUCh-5 scaffolds ($p < 0.01$, $p < 0.004$, and $p < 0.003$, respectively). Moreover, PUCh scaffolds didn't have statistical differences between themselves [Figure 6].

DISCUSSION

Intervertebral disc (IVD) degeneration is one of the prime causes of disability, and the present therapies are primarily far from satisfactory. Because scaffolds play a significant role in AF tissue engineering, their mechanical and biocompatibility properties should be noted deeply [28]. The current study for the first time reported the use of a 3D-printed PU scaffold coated with different content of Ch to improve the biocompatibility of the PU scaffold in AF tissue engineering applications.

SEM of PUCh scaffolds demonstrated that chitosan can improve the surface roughness of PU scaffolds. PU scaffold has a smooth and hydrophobicity surface and it is inappropriate for cell attachment and proliferation. Surface roughness enhances

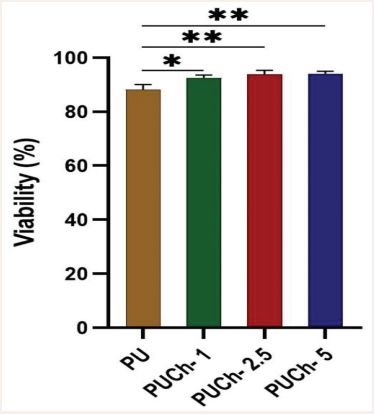

Figure 6 The viability rate of the scaffolds after 24 h via MTT test.
(*, p < 0.01; **, p < 0.004; **, p < 0.003).

cell attachment and proliferation, which in turn cells produce more collagen fibers and proteoglycans. Through increasing the mass of chitosan, the roughness and the space between PU fibers decreased, although it increased the hydrophilicity of the scaffold. Christiani and colleagues reported that 3D-printed PCL scaffolds, which were manually surface-modified with unidirectional grooves, demonstrated high roughness followed by improving cell attachment and deposition of collagen type I and aggrecan [29]. It should be considered that AF tissue, owing to its position in the body, receives a high level of stress and force that creates some small porosities or it drives them to be larger.

The mechanical performance of fabricated scaffolds is crucial for AF tissue engineering since it is under compression, stretching, and shearing stresses. The increase of chitosan content in PUCh scaffolds was consistent with the improvement of tensile strength (ranging from 0.61 to 0.72 MPa) and elastic modulus (1.16 to 1.25 MPa). However, it is far from the mechanical properties of native AF tissue, with tensile strength values between 4.0 and 6.8 MPa, and elastic modulus values between 4.5 and 6.8 MPa [30]. The scaffolds which were fabricated in our study had poor mechanical properties that could be because of many different reasons including (not limited to) poor connection between the struts, the number, and the thickness of the struts. It should be considered that the porosity structure affects the mechanical properties of a scaffold [31]. Zhao designed two different scaffolds from PCL based on the angle-ply architecture of native AF. The scaffold which had struts intersecting each other in a direction around 45° with the horizontal layer had higher mechanical strength than those which were designed based on traditional 3D scaffolds with struts at 90/0° to the horizontal layer 24. Similarly, our results showed that the scaffolds fabricated at 90/0°, had lower mechanical properties and it could be helpful to add oblique struts in our scaffolds in terms of improving mechanical properties. In another study, aligned (0°) and random electrospun scaffolds were fabricated through the electrospinning of polycarbonate urethane. The tensile strength of the aligned fiber scaffold (14 MPa) was significantly higher than the random fiber scaffold (1.9 MPa) [32]. Scaffold architecture must be considered when modifying mechanical properties and porosity to improve cell migration, attachment, proliferation, and endurance of in vivo loading [31]. The interconnected porous structure in the scaffold simplifies cell migration and diffusion to the depths of the scaffold, and cell communication. Moreover, the porous size in the scaffold should not be larger than the porous size of native AF tissue (401.4±13.1 μm) [33], because the mechanical strength will be reduced [34].

Porosity has an important role in biological properties and mostly natural polymers can have a direct impact on porosity. In this study, chitosan due to having a good swelling ratio, is applied to increase biological properties and porosity. Song in his study utilized hyaluronic acid (HA) to improve the biocompatibility of the Poly(lactide-co-glycolide) (PLGA) scaffold. The data indicated that the HA/PLGA scaffold (96.5 %) had a higher porosity than the PLGA scaffold (90.7 %) alone, although the porous size was smaller [35].

Biocompatibility and cellular interactions such as cell adhesion, differentiation, and proliferation are dependent on the hydrophilicity of coated materials on surfaces of scaffolds or medical devices [36]. The combination of functional groups like amines, carboxyls, and hydroxyls in chitosan influences the scaffolds' hydrophilicity, swelling ratio, cell attachment, and protein adsorption behaviour [37]. The fabricated PUCh scaffolds indicated a good swelling ratio and are appropriate for tissue engineering applications, which have been approved by previous studies that can facilitate cell attachment and growth. In a study, Nadhif indicated that the swelling ratio of TPU 87A and TPU 97A was 23.38% and 33.26%, respectively [38], while our study showed that through coating the PU scaffold with chitosan the swelling ratio significantly enhanced from 17% to 51 %. However, based on a study by Cortes, the swelling ratios of the scaffolds were significantly lower than the average swelling of human lumbar discs (142% under 1 kPa preload) [39]. However, scientists recommended other techniques to improve the swelling ratio. For instance, by embedding nanoparticles such as polydopamine within the scaffold's structure, the hydrophilicity properties of the scaffold can be improved [40].

In tissue-engineered scaffolds, the degradation rate must be in proportion to the regeneration rate [22]. PUCh scaffolds indicated a good rate of degradation compared to PU scaffolds. The degradation rate of PU scaffolds had a linear trend whereas PUCh scaffolds showed an exponential trend during 63 days (modeling was out of the study). Moreover, PUCh-2.5 appears to be degrading slowly and linearly, which suggests that the scaffolds will maintain the necessary physical integrity during neo-tissue formation. In contrast, PUCh-5 showed an initially rapid degradation until day 35, then became the same as PUCh-2.5. Comparing PU scaffold with PU scaffold coated with different amounts of chitosan, showed that chitosan is hypothesized to be the primary reason to change the initial degradation rate of PU scaffolds. Degradation of PU as an implanted scaffold must occur during a specific time in clinical settings. Due to its chemical structure, PU can be tailored for varying physiochemical properties such as degradation [41]. Guan et al., demonstrated that PU containing longer polyethylene glycol (PEG) blocks degraded to a greater extent than PU with shorter segments [42]. In a study, for IVD replacement, two types of thermoplastic PU (TPU) 3D printing filaments were used. The first group was pure TPU 87A, and the second one was TPU 95A containing adipic acid (50%), propyl isocyanate (30%), and 2–3-butanediol (20%). Although the degradation rate of TPU 97A was higher than pure TPU 87A, cell density in the latter, was lower than TPU 87A and control groups [38]. In this study, PU has been mixed with other materials while in our study, the PU scaffold was coated with chitosan which in turn, chitosan first starts to degrade, but in the previous study, PU and its mixed materials were predicted to degrade at the same time.

Cytocompatibility assessment is an essential step in the clinical translation of a biomaterial for tissue engineering applications. The fabricated 3D-printed constructs were tested for their cytocompatibility against fibroblast cells. The cytocompatibility

of the PUCh scaffolds showed a significant difference compared to the PU scaffold. In previous studies, it has been shown that chitosan had a good biocompatibility property, while PU, according to the proposed grade, has different biocompatibility properties. In this case, natural polymers are suggested to be used for improving biological properties. For example, similar to our study, Shaltooki reported that PCL scaffolds coated with chitosan had a higher viability rate than those without chitosan coating after 7 days of incubation against MG-63 cells [43]. In another study, Poddar et al., fabricated two different 3D scaffolds using PCL and chitosan. The first scaffold was fabricated by PCL and then coated with chitosan (C-PCL scaffold), while the second was made of a blend of PCL and chitosan (Chi-PCL). The results showed that the C-PCL scaffold enhanced cell attachment and proliferation behavior which, in turn, improved biocompatibility [44]. Based on the reports mentioned above, our approach in terms of biocompatibility was satisfactory and reasonable because of the chitosan properties such as swelling and water uptake. Nevertheless, it can be modified to enhance the biocompatibility feature.

CONCLUSION

The IVD is prone to damage and even failure due to injury, pathology, and aging. In this study, a chitosan-coated PU-based 3D bio-printed scaffold was fabricated for AF tissue engineering purposes. PU can be synthesized in different grads with distinct biological and biomechanical properties. Improving the mechanical strength of PU-based scaffolds reduces the biological properties. Thereby, coating the printed struts increased biocompatibility and bioavailability. Results showed that in the case of PU-based scaffolds for AF tissue engineering, the printed PU showed an appropriate mechanical strength. However, the PU scaffolds coated with chitosan could improve the scaffold biologically.

In recent years, several studies published focusing on engineering distinct scaffolds with alternative geometries and design. But still, it is challenging due to the complicated nature of AF. Based on our study, employing and evaluating various natural biomaterials will give more ideas about improving the biological properties of scaffolds. Surface modification without coating like linking of functional groups on the surface of the scaffolds or cold plasma can also help biological improvement in scaffolds.

Interestingly, it would be fascinating if, in the designed scaffolds for AF, a strategy for nucleus pulposus (NP) tissue engineering is considered. Certainly, this approach alters some resulting basics of AF tissue engineering. Meaning that an integration between AF and NP whether in the scaffold or after tissue regeneration will be a challenge for future studies.

Author Contribution

Mostafa Esmaeilpour (Project administration), Javad Esmaeili (conceptualization, methodology, paper editing), Mehdi Salehiamin (Project administration, writing drafts), Mitra Pakrouyan (Data analysis, writing drafts), Aboulfazl Barati (Supervision, paper editing)

REFERENCE

1. Yoshida M, Turner PR, Cabral JD. Intervertebral Disc Tissue Engineering Using Additive Manufacturing. Gels. 2022; 9: 25.
2. Wei Q, Liu D, Chu G, Yu Q, Liu Z, Li J, et al. TGF-β1-supplemented decellularized annulus fibrosus matrix hydrogels promote annulus fibrosus repair. Bioact Mater. 2023; 19: 581-593.
3. Liu C, Jin Z, Ge X, Zhang Y, Xu H. Decellularized Annulus Fibrosus Matrix/Chitosan Hybrid Hydrogels with Basic Fibroblast Growth Factor for Annulus Fibrosus Tissue Engineering. Tissue Eng Part A. 2019; 25: 1605-1613.
4. Constant C, Hom WW, Nehrbass D, Carmel EN, Albers CE, Deml M, et al. Comparison and optimization of sheep in vivo intervertebral disc injury model. JOR Spine. 2022; 5: e1198.
5. Page MI, Easley JT, Bonilla AF, Patel VV, Puttlitz CM. Biomechanical evaluation of a novel repair strategy for intervertebral disc herniation in an ovine lumbar spine model. Front Bioeng Biotechnol. 2022; 10: 1018257.
6. Distefano TJ, Shmukler JO, Danias G, Latridis JC. The Functional Role of Interface Tissue Engineering in Annulus Fibrosus Repair: Bridging Mechanisms of Hydrogel Integration with Regenerative Outcomes. ACS Biomater Sci Eng. 2020; 6: 6556-6586.
7. Gullbrand SE, Ashinsky BG, Bonnevie ED, Kim DH, Engiles JB, Smith LJ, et al. Long-term mechanical function and integration of an implanted tissue-engineered intervertebral disc. Sci Transl Med. 2018; 10: eaau0670.
8. Ashinsky BG, Gullbrand SE, Bonnevie ED, Wang C, Kim DH, Han L, et al. Sacrificial Fibers Improve Matrix Distribution and Micromechanical Properties in a Tissue-Engineered Intervertebral Disc. Acta Biomater. 2020; 111: 232–241.
9. Gullbrand SE, Kim DH, Ashinsky BG, Bonnevie ED, Smit HE, Mauck RL. Restoration of physiologic loading modulates engineered intervertebral disc structure and function in an in vivo model. JOR Spine. 2020; 3: e1086.
10. Kim HY, Kim HN, Lee SJ, Song JE, Kwon SY, Chung JW, et al. Effect of pore sizes of PLGA scaffolds on mechanical properties and cell behaviour for nucleus pulposus regeneration in vivo. J Tissue Eng Regen Med. 2017; 11: 44-57.
11. Ruan D-K, Xin H, Zhang C, Wang C, Xu C, Li C, et al. Experimental Intervertebral Disc Regeneration with Tissue-Engineered Composite in a Canine Model. Tissue Eng Part A. 2010; 16: 2381-2389.
12. Zhang Y, Tan W, Wu M, Sun J, Cao W, Zhou C-S, et al. Characterization and cytocompatibility of 3D porous biomimetic scaffold derived from rabbit nucleus pulposus tissue in vitro. J Mater Sci Mater Med. 2021; 32: 8.
13. Blanquer SBG, Sharifi S, Grijpma DW. Development of Poly(Trimethylene Carbonate) Network Implants for Annulus Fibrosus Tissue Engineering. J Appl Biomater Funct Mater. 2012; 10: 177–184.
14. Turner PR, Yoshida M, Ali MA,Cabral JD. Melt Electrowritten Sandwich Scaffold Technique Using Sulforhodamine B to Monitor Stem Cell Behavior. Tissue Eng Part C Methods. 2020; 26: 519-527.
15. Shamsah AH, Cartmell SH, Richardson SM, Bosworth LA. Tissue Engineering the Annulus Fibrosus Using 3D Rings of Electrospun PCL:PLLA Angle-Ply Nanofiber Sheets. Front Bioeng Biotechnol. 2020; 7: 437.
16. Du L, Yang Q, Zhang J, Zhu M, Ma X, Zhang Y, et al. Engineering a biomimetic integrated scaffold for intervertebral disc replacement. Mater Sci Eng C Mater Biol Appl. 2019; 96: 522–529.

17. Liu C, Li Y, Zhang Y, Xu H. The experimental study of regeneration of annulus fibrosus using decellularized annulus fibrosus matrix/poly(ether carbonate urethane)urea-blended fibrous scaffolds with varying elastic moduli. J Biomed Mater Res Part A. 2022; 110: 991-1003.

18. Wu D, Tan J, Yao L, Tian J, Luo B, Li L, et al. Customized composite intervertebral disc scaffolds by integrated 3D bioprinting for therapeutic implantation. Compos Part A Appl Sci Manuf. 2021; 147: 106468.

19. Zhang Y, Gao H, Luo H, Chen D, Zhou Z, Cao X. High strength HA-PEG/NAGA-Gelma double network hydrogel for annulus fibrosus rupture repair. Smart Mater Med. 2022; 3: 128-138.

20. Liu C, Xiao L, Zhang Y, Zhao Q, Xu H. Regeneration of annulus fibrosus tissue using a DAFM/PECUU-blended electrospun scaffold. J Biomater Sci Polym Ed. 2020; 31: 2347-2361.

21. Dewle A, Rakshasmare P, Srivastava A. A Polycaprolactone (PCL)-Supported Electrocompacted Aligned Collagen Type-I Patch for Annulus Fibrosus Repair and Regeneration. ACS Appl Bio Mater 2021; 4: 1238-1251.

22. Bhunia BK, Dey S, Bandyopadhyay A, Mandal BB. 3D printing of annulus fibrosus anatomical equivalents recapitulating angle-ply architecture for intervertebral disc replacement. Appl Mater Today. 2021; 23: 101031.

23. Chuah YJ, Wu Y, Chia YQ, Cheong ML, Joshua JJ, Kang Y, et al. The co-influence of hyaluronic acid and collagen on the development of an engineered annulus tissue model with bone marrow stromal cells. Biomed Mater. 2022; 17.

24. Liu Z, Wang H, Yuan Z, Wei Q, Han F, Chen A, et al. High-resolution 3D printing of angle-ply annulus fibrosus scaffolds for intervertebral disc regeneration. Biofabrication. 2022; 15.25.

25. Huang W, Xiao Y, Shi X. Construction of Electrospun Organic/Inorganic Hybrid Nanofibers for Drug Delivery and Tissue Engineering Applications. Adv Fiber Mater. 2019; 1: 32-45.

26. Li P, Fu L, Liao Z, Peng Y, Ning C, Gao C, et al. Chitosan hydrogel/3D-printed poly(ε-caprolactone) hybrid scaffold containing synovial mesenchymal stem cells for cartilage regeneration based on tetrahedral framework nucleic acid recruitment. Biomaterials. 2021; 278: 121131.

27. Nelson M, Li S, Page SJ, Shi X, Lee PD, Stevens MM, et al. 3D printed silica-gelatin hybrid scaffolds of specific channel sizes promote collagen Type II, Sox9 and Aggrecan production from chondrocytes. Mater Sci Eng C Mater Biol Appl. 2021; 123: 111964.

28. Gkantsinikoudis N, Kapetanakis S, Magras I, Tsiridis E, Kritis A. Tissue Engineering of Human Intervertebral Disc: A Concise Review. Tissue Eng Part B Rev. 2022; 28: 848-860.

29. Christiani TR, Baroncini E, Stanzione J, Vernengo AJ. In vitro evaluation of 3D printed polycaprolactone scaffolds with angle-ply architecture for annulus fibrosus tissue engineering. Regen Biomater. 2019; 6: 175-184.

30. Sharifi S, van Kooten TG, Kranenburg H-JC, Meij BP, Behl M, Lendlein A, et al. An annulus fibrosus closure device based on a biodegradable shape-memory polymer network. Biomaterials. 2013; 34: 8105–8113.

31. Harmon MD, Ramos DM, Nithyadevi D, Bordett R, Rudraiah S, Nukavarapu SP, et al. Growing a backbone – functional biomaterials and structures for intervertebral disc (IVD) repair and regeneration: challenges, innovations, and future directions. Biomater Sci. 2020; 8: 1216-1239.

32. Yeganegi M, Kandel RA, Santerre JP. Characterization of a biodegradable electrospun polyurethane nanofiber scaffold: Mechanical properties and cytotoxicity. Acta Biomater. 2010; 6: 3847-3855.

33. Wu YH, Xu BS, Yang Q, Li XL, Zhang Y, Ma XL, et al. Fabrication and Evaluation of a Novel Integrated Annulus Fibrosus-Nucleus Pulposus Hybrid Scaffold. Adv Mater Res 2013; 647: 688-691.

34. Zhu M, Tan J, Liu L, Tian J, Li L, Luo B, et al. Construction of biomimetic artificial intervertebral disc scaffold via 3D printing and electrospinning. Mater Sci Eng C Mater Biol Appl. 2021; 128: 112310.

35. Song JE, Kim MJ, Yoon H, Yoo H, Lee YJ, Kim HN, et al. Effect of hyaluronic acid (HA) in a HA/PLGA scaffold on annulus fibrosus regeneration: In vivo tests. Macromol Res. 2013; 21: 1075-1082.

36. Ghorbani F, Zamanian A, Aidun A. Bioinspired polydopamine coating-assisted electrospun polyurethane-graphene oxide nanofibers for bone tissue engineering application. J Appl Polym Sci. 2019; 136: 47656.

37. Poddar D, Jain P, Rawat S, Mohanty S. Influence of varying concentrations of chitosan coating on the pore wall of polycaprolactone based porous scaffolds for tissue engineering application. Carbohydr Polym. 2021; 259: 117501.

38. Nadhif MH, Ghiffary MM, Irsyad M, Mazfufah NF, Nurhaliza F, Rahman SF, et al. Anatomically and Biomechanically Relevant Monolithic Total Disc Replacement Made of 3D-Printed Thermoplastic Polyurethane. Polymers (Basel). 2022; 14: 4160.

39. Cortes DH, Jacobs NT, DeLucca JF, Elliott DM. Elastic, permeability and swelling properties of human intervertebral disc tissues: A benchmark for tissue engineering. J Biomech. 2014; 47: 2088-2094.

40. Ghorbani F, Ghalandari B, Khan AL,Li D, Zamanian A, Yu B. Decoration of electrical conductive polyurethane-polyaniline/polyvinyl alcohol matrixes with mussel-inspired polydopamine for bone tissue engineering. Biotechnol Prog. 2020; 36: e3043.

41. Hong Y, Guan J, Fujimoto KL, Hashizume R, Pelinescu AL, Wagner WR. Tailoring the degradation kinetics of poly (ester carbonate urethane) urea thermoplastic elastomers for tissue engineering scaffolds. Biomaterials. 2010; 31: 4249-4258.

42. Guan J, Sacks MS, Beckman EJ, Wagner WR. Biodegradable poly(ether ester urethane)urea elastomers based on poly(ether ester) triblock copolymers and putrescine: synthesis, characterization and cytocompatibility. Biomaterials. 2004; 25: 85-96.

43. Shaltooki M, Dini G, Mehdikhani M. Fabrication of chitosan-coated porous polycaprolactone/strontium-substituted bioactive glass nanocomposite scaffold for bone tissue engineering. Mater Sci Eng C Mater Biol Appl. 2019; 105: 110138.

44. Poddar D, Majood M, Singh A, Mohanty S, Jain P. Chitosan-coated pore wall polycaprolactone three-dimensional porous scaffolds fabricated by porogen leaching method for bone tissue engineering: a comparative study on blending technique to fabricate scaffolds. Prog Biomater. 2021; 10: 281-297..